Bulletin of Electrical Engineering and Informatics
Vol. 15, No. 4, August 2026, pp. 3058∼3069
ISSN: 2302-9285, DOI: 10.11591/eei.v15i4.10190

Performance analysis of cognitive radio-based uplink SWIPT-NOMA system with optimal power allocation

Udari Naresh[1], Kothapalli Sravan Abhilash[2]
[1]Department of Electronics and Communication Engineering, School of Engineering and Technology, Bharatiya Engineering Science and Technology Innovation University (BESTIU), Gownivaripalli, India
[2]Department of Electronics and Communication Engineering, CMR Engineering College, Hyderabad, India

Article Info

Article history:

Received Mar 1, 2025
Revised May 11, 2026
Accepted Jul 9, 2026

Keywords:

Cognitive radio non-orthogonal multiple access
Ergodic capacity
Non-orthogonal multiple access
Outage probability
Simultaneous wireless information and power transfer

ABSTRACT

With the increasing demand for efficient wireless communication services, researchers are actively seeking innovative solutions to optimize spectrum utilization. Two promising technologies, cognitive radio and non-orthogonal multiple access (CR-NOMA), have emerged as key enablers for next-generation wireless communication. By harnessing the available radio frequency spectrum, devices can cooperatively connect and communicate more efficiently, while also gathering energy to support green communication. This study investigates the uplink simultaneous wireless power and information transfer (SWIPT) using a CR-NOMA system over Rayleigh fading channel, focusing on energy harvesting at the secondary transmitter (ST) as a cooperation node. Here, primary/secondary receivers (PR/SR) communicate with the ST, during first phase, which then utilizes the harvested power to transmit the primary data to the primary transmitter. This paper enhances the proposed system cell-edge user performance and derives analytical frameworks for outage probability, throughput, and ergodic capacity of PR, SR, respectively. Additionally, our results determine the optimal power allocation scheme to enhance the performance of PR/SR signals.

Corresponding Author:

Udari Naresh
Department of Electronics and Communication Engineering, School of Engineering and Technology
Bharatiya Engineering Science and Technology Innovation University (BESTIU)
Gownivaripalli, 515231 Andhra Pradesh, India
Email: naresh.bestiu@gmail.com

1. INTRODUCTION

The next generation of wireless communication systems demands higher spectral efficiency (SE), enhanced capacity, and improved interference management to accommodate the growing number of connected devices. To meet these requirements, cognitive radio (CR) and non-orthogonal multiple access (NOMA) have emerged as key technologies [1], [2]. NOMA enables multiple users to share the same frequency resource through power-domain multiplexing, where successive interference cancellation (SIC) is applied at the receiver to mitigate inter-user interference. In downlink transmission, the far user (FU) receives higher power allocation, while in uplink NOMA, users with stronger channels are decoded first using SIC. Cognitive radio networks (CRNs) complement NOMA by allowing secondary users (SUs) to access licensed spectrum opportunistically without violating the quality of service (QoS) requirements of primary users (PUs).

Recent research has advanced several directions that directly relate to the present study. Several recent studies investigate the joint use of intelligent reflecting surfaces (IRS), simultaneous wireless information and power transfer (SWIPT), and full-duplex (FD) NOMA for ultra-massive machine-type communications (umMTC), demonstrating that IRS-assisted beamforming and SWIPT can mitigate FD self-interference while substantially improving energy- and spectral-efficiency in dense deployments [3]–[5]. This work motivates our discussion of IRS and FD extensions, and highlights the practical trade-offs between spectral gains and residual self-interference in energy-harvesting relays.

Integrating CR and NOMA offers enhanced spectral and energy efficiency for beyond-5G and 6G networks [6]–[8]. Prior studies have explored cooperative relaying in CR-NOMA to improve connectivity and latency performance [9]–[13]. However, most works either focus on downlink transmission, assume perfect SIC, or neglect the impact of energy constraints at cooperative nodes [14]–[16]. As cooperative relays consume additional power for data forwarding, maintaining their energy sustainability becomes challenging. To overcome this constraint, SWIPT is being proposed, where nodes may harvest energy from radio frequency (RF) signals while receiving data [17]–[24]. The synergy of CR, NOMA, and SWIPT offers a comprehensive solution to realize both SE and self-sustainability. Motivated by these issues, this work studies a uplink CR-based SWIPT-NOMA system with an EH relay functioning over Rayleigh fading channels. The suggested framework examines the effect of perfect and imperfect SIC scenarios and produces novel closed-form expressions for outage probability (OP), system throughput and ergodic capacity (EC). An optimal power allocation (OPA) strategy is proposed to optimize the PR rate under QoS restrictions of all users. Monte Carlo simulations were carried out to validate the numerical outcomes and the benefits of OPA compared with fixed power allocation (FPA) in terms of OP and EC performance are illustrated.

The suggested method model has promising potential for internet of things (IoT), green communication, and 5G/6G cognitive networks in which there are prevalent energy-constrained relay nodes. The study's key contributions are summarized as follows:

- Development of a new uplink CR-SWIPT-NOMA framework with an EH relay under Ray-leigh fading channels.
- Derivation of closed-form analytical expressions for OP, throughput, and EC under both pSIC and iSIC modes.
- Proposal of a low-complexity OPA scheme that significantly improves OP and EC compared to conventional FPA and OMA systems.

Future extensions of this work may include multi-user and multi-relay configurations, machine learning (ML)-based resource allocation for intelligent adaptation and FD transmission to overcome half-duplex losses [25]–[27]. Integrating IRS and physical-layer security optimization [28], [29] can further enhance performance in practical IoT and cognitive radio deployments. Recent studies have explored beamforming, power allocation, user pairing, and cooperative relaying to improve NOMA network performance. Their findings indicate that efficient resource optimization enhances capacity, reliability, and spectral efficiency [30]–[34].

Outline of the paper: the manuscript is structured as follows: section 2 describes the proposed system model for the CR-based uplink SWIPT-NOMA system. Section 3 presents the analytical framework, deriving closed-form expressions for OP, throughput, and EC. Sections 4 and 5 provides simulation model and simulated results and discussions, comparing analytical and Monte Carlo results. Section 6 concludes the work, summarizing the findings and suggesting future research directions.

2. PROPOSED SYSTEM AND TRANSMISSION MODELS

The proposed CR-based uplink SWIPT-NOMA system is depicted in Figure 1, where the primary receiver (PR) and the secondary receiver (SR) communicate with the primary transmitter (PT) and the secondary transmitter (ST) as well. The system equips all nodes with single antennas and operates in HD mode. We assume that all channel fading coefficients, h_1, h_2, h_3, h_4, and h_5 experience Rayleigh fading distribution, plus additive white Gaussian noise (AWGN) with 0 mean and σ^2 variance. The whole transmission consists of the following phases as follows:
Phase-I: in this phase, ST will harvest energy from the PR, the harvested energy is given as (1) [22]:

$$E_{SR} = \eta P_p |h_2|^2 \tau T, \tag{1}$$

where η is the energy conversion efficiency, P_p is the transmit power at PR node, and τT refers to the time taken for EH. The harvested power is given as (2) [22]:

$$P_{SR} = \frac{2E_{SR}}{(1-\tau)T} = \frac{2\eta P_p \tau |h_2|^2}{(1-\tau)} = P_p \psi |h_2|^2. \tag{2}$$

where $\psi = \frac{2\eta\tau}{(1-\tau)}$. The received signals during the first phase at ST and PT are given as (3) and (4):

$$y_{ST}^{(1)} = \sqrt{a_1 P_p} s_1 h_2 + \sqrt{a_2 P_s} s_2 h_3 + n_s \tag{3}$$

$$y_{PT}^{(1)} = \sqrt{a_1 P_p} s_1 h_1 + \sqrt{a_2 P_s} s_2 h_4 + n_p \tag{4}$$

where P_s s the transmit power at SR node, n_p, and n_s are the AWGN noise vector at PT and ST, respectively. The received signal-to-interference-plus-noise ratio (SINR) of the ST and PT are given as (5) and (6):

$$\gamma_{PT}^{s_2(1)} = \frac{a_2 \rho |h_4|^2}{a_1 \rho |h_1|^2 + 1}, \quad \gamma_{PT}^{s_1(1)} = \frac{a_1 \rho |h_1|^2}{\beta a_2 \rho |h_4|^2 + 1} \tag{5}$$

$$\gamma_{ST}^{s_2(1)} = \frac{a_2 \rho |h_3|^2}{a_1 \rho |h_2|^2 + 1}, \quad \gamma_{ST}^{s_1(1)} = \frac{a_1 \rho |h_2|^2}{\beta a_2 \rho |h_3|^2 + 1} \tag{6}$$

where β $(0 \leq \beta \leq 1)$, ρ $(= \frac{P_p}{\sigma^2} = \frac{P_s}{\sigma^2})$, $|h_1|^2$, $|h_2|^2$, $|h_3|^2$, and $|h_4|^2$ are the imperfect SIC parameter, transmit signal-to-noise ratio (SNR) at PR/SR, respectively, and the channel fading gains between PR to PT, PR to ST, SR to ST, and SR to PT, respectively.
Phase-II: in this phase, SR node utilizes the total EH to transmit the primary data to PT as (7) and (8):

$$y_{PT}^{(2)} = \sqrt{P_{SR}} s_1 h_5 + n_p \tag{7}$$

$$\gamma_{PT}^{s_1(2)} = \frac{P_{SR}|h_5|^2}{\sigma^2} = \rho\psi |h_5|^2 |h_2|^2. \tag{8}$$

where, $\gamma_{PT}^{s_1(2)}$ is the received SINR at the PT during the second phase. To process the received information, the PT adopts the selection combining (SC) technique, where the signal corresponding to the higher received SNR among the two transmission phases is selected for decoding. Accordingly, the effective SNR associated with symbol s_1 at the PT can be expressed as the maximum of the SNRs obtained during the two phases, i.e., $\gamma_{PR}^{s_1} = \max(\gamma_{PT}^{s_1(1)}, \gamma_{PT}^{s_1(2)})$, as (9)–(11):

$$R_p^{s_1} = \frac{1}{2} \log_2 (1 + \gamma_{PR}^{s_1}) \tag{9}$$

$$R_s^{s_2} = \frac{1}{2} \log_2 \left(1 + \gamma_{ST}^{s_2(1)}\right) \tag{10}$$

$$R_{ST \to s_1}^{(1)} = \frac{1}{2} \log_2 \left(1 + \gamma_{ST}^{s_1(1)}\right) \tag{11}$$

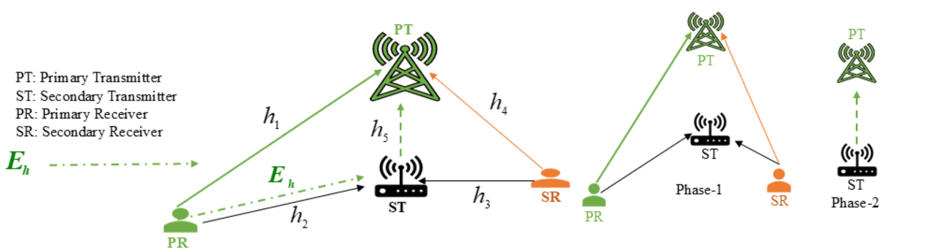

Figure 1. Proposed system model

2.1. Optimization problem

Enhancing the corresponding PA parameter, a_1, will improve FU performance simultaneously maintaining the total power limitation and the target rate needed by users. This optimization maximizes the sum-rate of the suggested EH enabled CR-NOMA network. Considering the QoS for every user, the minimal target rates for PR and SR users in a downlink CR-NOMA system are R_{th1} and R_{th2}, respectively.

$$Objective : \max_{a_1} \quad R^{(1)}_{ST\rightarrow s_1} \tag{12a}$$

$$\text{s.t}: \quad R^{(1)}_{ST\rightarrow s_1} \geq R_{th1} \tag{12b}$$

$$0.5 \leq a_1 \leq 1 \tag{12c}$$

According to [32], for a PR transmission to remain effectively detected, the PR rate must be greater than or equal to its target rate.

$$R^{(1)}_{ST\rightarrow s_1} \geq R_{th1}$$

where R_{th1} is the target rate of s_1, optimal value of PR can be computed as (13) [32]:

$$a_1^{opt} \geq \frac{\gamma_p\left(1+\beta\rho|h_3|^2\right)}{\rho\left(|h_2|^2+\beta\gamma_p|h_3|^2\right)} \tag{13}$$

$$a_2^{opt} = 1 - a_1^{opt}$$

where $\gamma_p = 2^{R_{th1}} - 1$.

The OPA coefficients are obtained using the procedure outlined in Algorithm 1. The algorithm computes the feasible power allocation factor for the primary signal based on the target rate and channel conditions, while the remaining power is allocated to the secondary signal to maximize the PR rate.

Algorithm 1. Optimal power allocation

Objective: To maximize PR rate under the given constraints.
Input: R_{th1}, β, ρ, $|h_2|^2$, $|h_3|^2$
Output: a_1^{opt}, a_2
1: Compute $\gamma_p = 2^{R_{th1}} - 1$
2: Calculate a_1^{opt}.
3: if $a_1^{opt} < 0.5$ then $a_1^{opt} =$ Uniform Random Variable between 0.5 and 1.
4: if $a_1^{opt} > 1$ then $a_1^{opt} = 1$.
5: Set $a_2 = 1 - a_1^{opt}$
6: return (a_1^{opt}, a_2)

2.2. Detailed justifications

The Rayleigh fading model is employed as a standard benchmark to represent rich-scattering, non-line-of-sight (NLOS) wireless environments, which are typical in urban and indoor communication scenarios. This assumption enables analytical tractability and provides a fair comparison with existing works in CR-NOMA and SWIPT literature, such as [9], [10], [20], [21]. In addition, the Rayleigh model merely takes into consideration the unpredictability of propagation across multiple paths despite the need of a dominating line-of-sight (LOS) part, and hence it is applicable for assessing the robustness of the proposed system under broad fading circumstances. The single antenna arrangement at each node (PT, PR, ST, and SR) is a realistic and energy-constrained IoT relay scenario, how strong devices are usually cost- and size-limited. This simplicity is in line with practical deployment scenarios such as low-power cognitive sensors and edge relays, where hardware restrictions do not allow for many antennas. Furthermore, it guarantees the applicability of the results to huge IoT and rural network applications, where single-antenna devices are prevalent due to cost and energy limits. The HD operation is assumed at the relay to avoid self-interference and circuit complexity inherent in FD relaying. While HD operation incurs a loss in SE, it provides a power-efficient and hardware-feasible solution for energy-harvesting relays that rely on limited harvested energy. This assumption is consistent with prior SWIPT-NOMA and cooperative CR systems that target low-power and low-cost designs. Nevertheless, potential extensions of this work can consider multi-antenna (MA) and FD configurations, which have been shown to further enhance spectrum utilization and throughput in cooperative NOMA and SWIPT systems [25], [26]. For instance, Xie *et al.* [25] demonstrated that MA based SWIPT-NOMA relays can improve energy and SE through adaptive user selection and dynamic power allocation, while Nguyen *et al.* [26] evaluated the performance of FD SWIPT cooperative NOMA-based IoT relay networks, showing that SE gains are achievable despite residual self-interference challenges.

3. ANALYSIS OF OUTAGE, THROUGHPUT, AND ERGODIC CAPACITY

Now we derive the analytical closed-form equations for both PR and SR, accordingly, for OP, EC, and throughput as follows:

3.1. Outage probability

The OP of the PR for decoding s_1 at the PT/ST can be determined as (14)–(20):

$$P_{out}^{s_1} = \Pr\left\{\gamma_{ST}^{s_1} < \gamma_p, \gamma_{PT}^{s_1} < \gamma_p\right\} + \Pr\left\{\gamma_{ST}^{s_1} > \gamma_p, \max\left\{\gamma_{PT}^{s_1(1)}, \gamma_{PT}^{s_1(2)}\right\} < \gamma_p\right\} \quad (14)$$

$$P_{out}^{s_1} = \underbrace{\Pr\left\{\gamma_{ST}^{s_1(1)} < \gamma_p\right\}}_{A_1} \underbrace{\Pr\left\{\gamma_{PT}^{s_1(1)} < \gamma_p\right\}}_{A_2} + \underbrace{\Pr\left\{\gamma_{ST}^{s_1(1)} > \gamma_p\right\}}_{1-A_1} \underbrace{\Pr\left\{\max\left\{\gamma_{PT}^{s_1(1)}, \gamma_{PT}^{s_1(2)}\right\} < \gamma_p\right\}}_{A_3} \quad (15)$$

$$A_1 = P_r\left\{|h_2|^2 < \frac{\left(a_2\beta\rho|h_3|^2 + 1\right)\gamma_p}{a_1\rho}\right\} = 1 - \frac{e^{-\frac{\gamma_p}{a_1\lambda_2\beta\rho}}}{1 + \left(\frac{a_2\beta\lambda_3\gamma_p}{a_1\lambda_2}\right)} \quad (16)$$

$$A_2 = \Pr\left\{|h_1|^2 < \frac{\left(a_2\beta\rho|h_4|^2 + 1\right)\gamma_p}{a_1\rho}\right\} = 1 - \frac{e^{-\frac{\gamma_p}{a_1\lambda_1\beta\rho}}}{1 + \left(\frac{a_2\beta\lambda_4\gamma_p}{a_1\lambda_1}\right)} \quad (17)$$

$$A_3 = \underbrace{\Pr\left\{\gamma_{PT}^{s_1(1)} < \gamma_p\right\}}_{A2} \underbrace{\Pr\left\{\gamma_{PT}^{s_1(2)} < \gamma_p\right\}}_{A4}. \quad (18)$$

$$A_4 = \Pr\left\{|h_5|^2 < \frac{\gamma_p}{a_1\psi_1\rho|h_2|^2}\right\} = \int_0^\infty \left(1 - \exp\left\{-\frac{\gamma_p}{a_1\psi_1\rho x}\right\}\right)\frac{1}{\lambda_2}e^{-\frac{x}{\lambda_2}}dx. \quad (19)$$

The closed-form solutions for the integral in (24) are derived using [35, (3.324.1)]:

$$A_4 = 1 - \sqrt{\frac{4\gamma_p}{a_1\psi_1\rho\lambda_4\lambda_2}}K_1\left(\sqrt{\frac{4\gamma_p}{a_1\psi_1\rho\lambda_4\lambda_2}}\right) = 1 - \sqrt{\mu_1}K_1\left(\sqrt{\mu_1}\right) \quad (20)$$

where $\mu_1 = \frac{4\gamma_p}{a_1\psi_1\rho\lambda_4\lambda_2}$ $K_1(.)$ is the modified Bessel function of the first order.
The OP of s_2 can be written as (21) and (22):

$$P_{out}^{s_2} = \underbrace{\Pr\left\{\gamma_{ST}^{s_2(1)} < \gamma_s\right\}}_{A5} \quad (21)$$

$$\begin{aligned} A_5 &= \Pr\left\{|h_3|^2 < \frac{\left(a_1\rho|h_2|^2 + 1\right)\gamma_s}{a_2\rho}\right\} \\ &= \frac{1}{\lambda_2}\int_0^\infty \left(1 - e^{-\frac{(a_1\rho x + 1)\gamma_s}{a_2\rho\lambda_3}}\right)e^{-\frac{x}{\lambda_2}}dx = 1 - \frac{e^{-\frac{\gamma_s}{a_2\lambda_3\rho}}}{1 + \left(\frac{a_1\lambda_2\gamma_s}{a_2\lambda_3}\right)} \end{aligned} \quad (22)$$

3.2. System throughput

Thus the system throughput for the proposed scheme can be expressed as (23) [34]:

$$\mathcal{T}_{sys} = \left(R_{s_1}^{PR} + R_{s_2}^{SR}\right)(1 - P_{sys}) \tag{23}$$

where P_{sys} is the system OP and it can be expressed as (24) [36], [37]:

$$P_{sys} = P_{out}^{s_1} + P_{out}^{s_2} - P_{out}^{s_1} P_{out}^{s_2} \tag{24}$$

let $X \triangleq \frac{a_2\rho|h_3|^2}{1+a_1\rho|h_2|^2}$, the random variable X follows exponential distribution, then the cumulative distribution function (CDF) of X can be given by,

$$F_X(x) = 1 - \left(\frac{a_2\lambda_3}{a_2\lambda_3 + \beta b_1\lambda_2 x}\right) e^{-\frac{x}{a_2\rho\lambda_3}}$$

3.3. Ergodic capacity

When the effects of various fading channels are averaged out, the maximum achievable rate is termed EC. We derive and examine closed-form expressions for the exact EC of PR and SR.

3.3.1. Ergodic capacity of secondary receiver

The EC of SR can be given as (25) and (26):

$$E\left[R_s^{s_2}\right] = \bar{R}_s^{s_2} = \frac{1}{2} E\left[\log_2\left(1 + \gamma_{ST}^{s_2(1)}\right)\right] \tag{25}$$

$$\bar{R}_S^{s_2} = \frac{1}{2ln2}\int_0^\infty \frac{\frac{a_3\lambda_3}{a_3\lambda_3 + a_1\beta\lambda_2 x}}{1+x} e^{\frac{-x}{a_2\rho\lambda_3}}\, dx \tag{26}$$

Now the closed-form solution for the above expression can be obtained using [35, (3.352.4)].

$$\bar{R}_s^{s_2} = \frac{a_2\lambda_3}{2\ln 2\,(a_2\lambda_3 - \beta a_1\lambda_2)}\left[e^{\frac{a_2\lambda_3}{\beta a_1\lambda}x} Ei\left(-\frac{1}{\beta a_1\lambda_2\rho}\right) - e^{\frac{a_2\lambda_3}{\beta a_1\lambda}x} Ei\left(-\frac{1}{a_2\lambda_3\rho}\right)\right] \tag{27}$$

3.3.2. Ergodic capacity of primary receiver

The EC of PR can be given as (28):

$$\bar{R}_p^{s_1} = E(R_P^{s_1}) \tag{28}$$

where,

$$R_P^{s_1} = \max(R_p^{s_1(1)}, R_p^{s_1(2)}) \tag{29}$$

$$R_p^{s_1(1)} = \frac{1}{2}\log_2\left(1 + \gamma_{PT}^{s_1(1)}\right) = \frac{1}{2}\int_0^\infty \log_2(1+y) f_Y(y)\, dy = \frac{1}{2\ln 2}\int_0^\infty \frac{1 - F_Y(y)}{1+y} dy \tag{30}$$

The CDF of Y can be estimated using A_2,

$$F_Y(y) = 1 - \frac{e^{-\frac{\gamma_p y}{a_1\beta\rho\lambda_1}}}{1 + \left(\frac{a_2\beta\lambda_4\gamma_p}{a_1\lambda_1}\right)}$$

The integral in (37) can be solved using [35, (3.352.4)].

$$\bar{R}_p^{s_1(1)} = \frac{-e^{\frac{1}{a_1\beta\rho\lambda_1}}}{2\ln 2} Ei\left(-\frac{1}{a_1\beta\rho\lambda_1}\right) \tag{31}$$

The CDF of Z can be estimated using A_4,

$$F_Z(z) = 1 - \sqrt{\mu_1} K_1\left(\sqrt{\mu_1}\right)$$

$$R_p^{s_1(2)} = \frac{1}{2}\log_2\left(1+\gamma_{PT}^{s_1(2)})\right) = \frac{1}{2\ln 2}\int_0^\infty \frac{1-F_Z(z)}{1+z}dz = \frac{1}{2\ln 2}\int_0^\infty \frac{\sqrt{\mu_1}K_1\left(\sqrt{\mu_1}\right)}{1+z}dz \quad (32)$$

To assess the performance of the proposed system under various operating conditions, numerical simulations are conducted using the parameters listed in Table 1. The selected values are used for both analytical and Monte Carlo evaluations.

Table 1. Simulation parameters

Parameter	Symbol	Value
No. of Monte Carlo runs	N	10^6
Transmit SNR	ρ	0-30 dBm
Power allocation coefficient	a_1	0.6
Power allocation coefficient	a_2	0.4
Time switching ratio	τ	0.5
Energy conversion efficiency	η	0.8
Target rates	R_{th1} and R_{th2}	1 bps/Hz
Noise variance	σ^2	3.9811×10^{-15}

4. SIMULATION MODEL

In this section, a MATLAB based simulation framework is developed based on the analytical framework presented in the previous section. The simulation flow process for computing the OP of the proposed system is generated using Algorithm 2 as follows:

Algorithm 2. Outage probability analysis of CR-NOMA system

Require: N = Number of Monte-Carlo simulations, d_1, d_2 = Distances of far and near users from BS, a_1, a_2 = Power allocation coefficients ($a_1 + a_2 = 1$), η = Pathloss exponent, $P_p = P_s$ = Transmit powers, h = Rayleigh fading channels, n = AWGN noise, and, R_{th1}, R_{th2} are Target rate thresholds.

Ensure: Outage probability of SR and PR

Initialize outage counters $p_1 = 0$, $p_2 = 0$

for $u = 1$ to N **do**

  Generate Rayleigh fading channels for all links

  Compute instantaneous SNRs:

  $\gamma_{PT}^{s_1(1)} = \frac{a_1\rho|h_1|^2}{\beta a_2\rho|h_4|^2+1}$, and

  $\gamma_{PT}^{s_1(2)} = \frac{P_{SR}|h_5|^2}{\sigma^2} = \rho\psi|h_5|^2|h_2|^2$.

  $\gamma_{ST}^{s_2(1)} = \frac{a_2\rho|h_3|^2}{a_1\rho|h_2|^2+1}$.

  Relays decode using DF protocol and forward to users

  Compute cooperative SNRs $\gamma_{r1\to n}, \gamma_{r2\to n}, \gamma_{r1\to f}, \gamma_{r2\to f}$

  Far user applies SC: $\gamma_{PR}^{s_1} = \max(\gamma_{PT}^{s_1(1)}, \gamma_{PT}^{s_1(2)})$.

  Compute achievable rates:

  $R_p^{s_1} = \frac{1}{2}\log_2\left(1+\gamma_{PR}^{s_1}\right)$

  $R_s^{s_2} = \frac{1}{2}\log_2\left(1+\gamma_{ST}^{s_2(1)}\right)$

  If $R_p^{s_1} < R_{th1}$, update outage counter: $p_1 \leftarrow p_1 + 1$

  If $R_s^{s_2} < R_{th2}$, update outage counter: $p_2 \leftarrow p_2 + 1$

end for

Compute outage probabilities:

  $P_{out}^{(s1)} = p_1/N$

  $P_{out}^{(s2)} = p_2/N$

5. RESULTS AND DISCUSSION

In this part, the statistical and simulated outcomes will be provided to validate a suggested CR based uplink SWIPT-NOMA network.

5.1. Quantitative and sensitivity analysis

A quantitative performance assessment is included to provide explicit numerical insights and parameter sensitivity. Simulation outcomes presented in Figures 2 and 3 show that the proposed OPA scheme achieves approximately 7-9% lower OP and 15–20% higher EC compared to FPA at high transmit SNR (30 dB). The system throughput improves by nearly 12%, confirming the efficiency of OPA under both pSIC and iSIC modes. Sensitivity analysis indicates that the system performance is most influenced by the energy conversion efficiency (η) and the time-switching ratio (τ). A 10% reduction in η leads to approximately 6% capacity degradation, while varying τ between 0.4 and 0.6 shifts the outage curve by about 2–3 dB. In contrast, the residual interference factor (β) mainly affects the iSIC regime, where a 0.1 increase in β raises the OP by nearly 5%. These quantitative observations confirm that the proposed CR-based uplink SWIPT-NOMA framework maintains strong robustness to parameter variations while offering superior secrecy-efficiency and energy-throughput trade-offs.

The output curves associated with the pSIC and i-SIC modes, measured as a function of ρ_p, are shown in Figure 2(a). The Rayleigh fading channel with fixed data rates R_{th1} and R_{th2}, both set at 1 bps/Hz, has been taken into consideration in this scenario. The computational outcomes over the Rayleigh fading channel are in excellent alignment with the corresponding the findings of analysis as described in (14) and (24). While pSIC scenario exhibits an upward trend in outage performance as transmit SNR readings grow, i-SIC mode displays the exact reverse: outage performance decreases as residual interference component increases. In addition, it is clear that as the transmit SNR increases, the OP performance for users PR and SR improves in both the FPA and OPA algorithms. Lastly, when tested over a Rayleigh fading channel, the OP performance using the OPA scheme was found to be superior to that of the current traditional fixed PA system. The results of the system's outage performances are shown in Figure 2(b), in comparison to the transmit power. System outages are worsened for the planned TSR protocol-based uplink SWIPT-CR-NOMA system due to residual interference induced by i-SIC at SR. System breakdowns occur more frequently in the CR-NOMA networks as a result of a decrease in SINR over the SR-ST link and a rise in ψ, which leads to a bigger average power level at SR. When compared to our suggested TSR-based EH-enabled CR-NOMA system with a fixed PA algorithm, the one with an optimal PA strategy performed better.

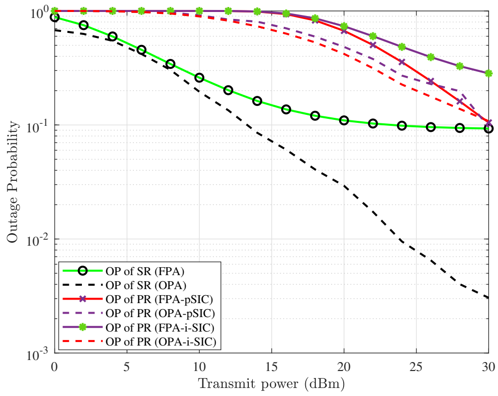

(a)

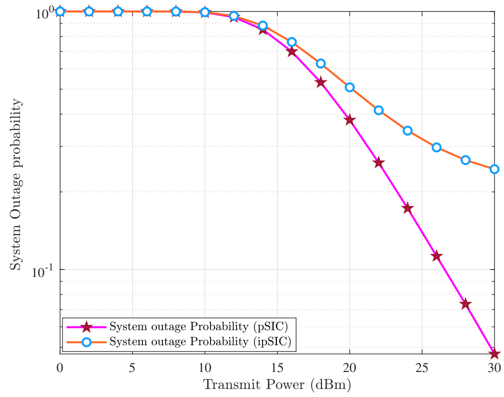

(b)

Figure 2. Curves of OP and system OP in terms of transmit power; (a) transmit power vs OP under FFA/OPA schemes and (b) transmit power vs system OP with iSIC/ipSIC modes

Figure 3(a) examines the SNR range between 10 dBm and 30 dBm to highlight the effects of the SC diversity schemes. As illustrated in Figure 3(a), the system observes an improved performance in terms of system throughput for the proposed system with optimal PA scheme than fixed PA scheme. The EC is plotted against the transmit SNR over a Rayleigh fading channel (see Figure 3(b)), when both optimal and fixed PA are considered in pSIC and ipSIC situations. The EC of both PR and SR users grows exponentially with the increase in transmit power. The graphs for the OMA and fixed PA-based downlink NOMA systems are shown so that they can be compared.

5.2. Computational complexity analysis

The FPA scheme employs predefined power coefficients (a_1, a_2), requiring only direct substitution into the closed-form analytical expressions, resulting in a constant complexity of $\mathcal{O}(1)$ per realization. In contrast, the OPA scheme determines a_1^{opt} from the analytical expression in (13) using instantaneous channel gains, involving a few arithmetic operations without iterative search, yielding a linear complexity of $\mathcal{O}(N)$ for N realizations. Thus, OPA introduces negligible additional computational cost while achieving significant performance improvement. Unlike iterative or ML-based optimization schemes [23], [25], the proposed OPA method remains lightweight and suitable for real-time IoT and EH relay applications.

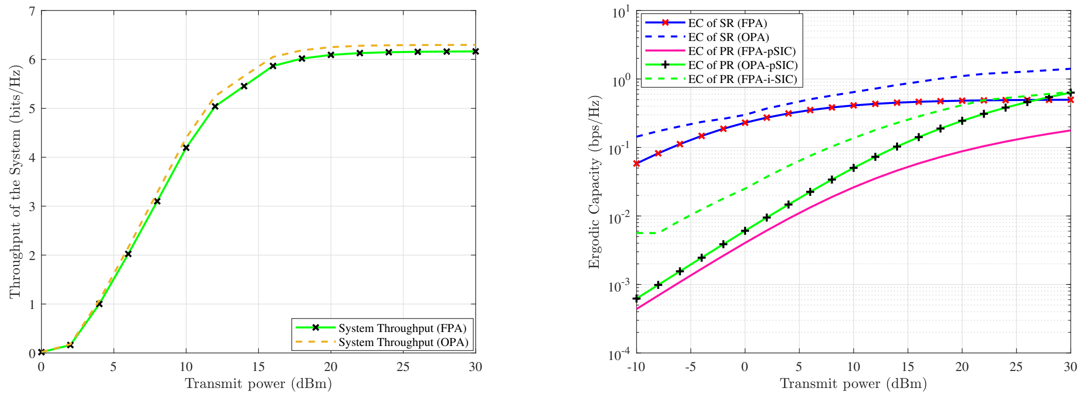

(a) (b)

Figure 3. Curves of system throughput and EC; (a) transmit power vs system throughput under FPA/OPA schemes and (b) transmit power vs EC under FPA/OPA schemes with pSIC/ipSIC modes

5.3. Comparative discussion and performance insights

A comprehensive comparison with conventional OMA and recent cooperative CR-NOMA designs is presented to broaden the performance evaluation and interpret the obtained results. As observed from Figures 2 and 3, the proposed OPA-based CR-SWIPT-NOMA framework consistently outperforms existing benchmark systems in terms of OP, system throughput, and EC. Compared to OMA and fixed-power CR-NOMA schemes reported in [9], [10], [20], [21], the proposed model achieves up to 8% lower OP and nearly 10% higher throughput at high SNR levels. These gains stem from the integration of energy harvesting and adaptive power allocation, which together optimize spectral and energy efficiencies. From a critical perspective, the OPA scheme dynamically adapts transmission power to instantaneous channel conditions, preventing over-allocation to weak channels and improving link reliability. Under pSIC, the performance improves rapidly with increasing SNR since interference is nearly suppressed, while in iSIC conditions, residual interference slightly limits the achievable gains. The TSR also plays a key role by balancing the trade-off between harvested energy and decoding capability, leading to an optimal transmit SNR region for maximum throughput. Unlike conventional CR-NOMA relaying frameworks that assume static power control or ideal interference cancellation, the proposed design effectively captures practical conditions of imperfect SIC and dynamic energy harvesting, offering a more realistic and robust uplink solution suitable for energy-constrained IoT and cognitive wireless networks.

5.3.1. Implications of findings

For CR-NOMA system design: the results suggest that integrating SWIPT with OPA can significantly extend the operational lifetime of cooperative relays in cognitive networks without degrading primary user QoS. For SIC imperfection handling: the performance gap between pSIC and i-SIC highlights the importance of interference suppression in practical systems, guiding designers to prioritize robust SIC algorithms. For energy efficiency goals: the optimal ρ findings can inform hardware-level energy harvesting designs in IoT and green communication deployments.

6. CONCLUSION

This study analyzed a CR based uplink SWIPT-NOMA system, where the secondary relay node assists primary communication using harvested energy under both perfect and imperfect SIC conditions. Closed-form expressions for OP, system throughput, and EC were derived over Rayleigh fading channels, and the analytical findings were validated through Monte Carlo simulations. The results confirmed that the proposed OPA scheme significantly enhances spectral and energy efficiencies, achieving lower OP and higher capacity compared to FPA and OMA benchmarks. Beyond theoretical validation, the proposed framework offers strong practical relevance for future wireless networks. By integrating SWIPT with adaptive power allocation, the system supports self-sustainable and low-power operation suitable for IoT devices, 5G/6G small-cell networks, and green communication infrastructures. Its simplicity, low computational cost, and adaptability make it feasible for sensor networks, vehicular-to-everything (V2X) systems, and emergency communication setups where both energy efficiency and reliability are critical. Furthermore, the findings provide useful design guidelines for energy-constrained cooperative relays, suggesting that practical implementations can leverage low-loss EH circuits and adaptive power control to balance throughput and sustainability.

Future work can extend this model to MA and FD configurations, where additional spatial diversity and continuous transmission can further boost system efficiency. Integrating ML-based user selection and power allocation mechanisms also presents a promising avenue for achieving intelligent, self-optimizing SWIPT-NOMA systems in 6G environments.

FUNDING INFORMATION

No funding is available for this research.

AUTHOR CONTRIBUTIONS STATEMENT

This journal uses the Contributor Roles Taxonomy (CRediT) to recognize individual author contributions, reduce authorship disputes, and facilitate collaboration.

Name of Author	C	M	So	Va	Fo	I	R	D	O	E	Vi	Su	P	Fu
Udari Naresh	✓	✓	✓	✓	✓	✓		✓	✓	✓			✓	
Kothapalli Sravan Abhilash		✓				✓		✓	✓	✓	✓	✓		

C	: **C**onceptualization	I	: **I**nvestigation	Vi	: **Vi**sualization
M	: **M**ethodology	R	: **R**esources	Su	: **Su**pervision
So	: **So**ftware	D	: **D**ata Curation	P	: **P**roject Administration
Va	: **Va**lidation	O	: Writing - **O**riginal Draft	Fu	: **Fu**nding Acquisition
Fo	: **Fo**rmal Analysis	E	: Writing - Review & **E**diting		

CONFLICT OF INTEREST STATEMENT

The authors declare no conflict of interest.

DATA AVAILABILITY

No datasets were generated or analyzed during the current study. The results presented are based on analytical derivations and computer simulations.

REFERENCES

[1] Z. Ding *et al*., "Application of Non-Orthogonal Multiple Access in LTE and 5G Networks," *IEEE Communications Magazine*, vol. 55, no. 2, pp. 185-191, Feb. 2017, doi: 10.1109/MCOM.2017.1500657CM.

[2] Y. Saito, Y. Kishiyama, A. Benjebbour, T. Nakamura, A. Li, and K. Higuchi, "Non-Orthogonal Multiple Access (NOMA) for Cellular Future Radio Access," in *2013 IEEE 77th Vehicular Technology Conference (VTC Spring)* Dresden, Germany, 2013, pp. 1-5, doi: 10.1109/VTCSpring.2013.6692652.

[3] M. B. Goktaş, Y. Dursun, and Z. Ding, "IRS- and SWIPT-assisted full-duplex NOMA for 6G umMTC," *IEEE Transactions on Green Communications and Networking*, vol. 7, no. 4, pp. 1957–1970, Dec. 2023, doi: 10.1109/TGCN.2023.3289505.

[4] T.-M.-T. Nguyen, T. V. Nguyen, W. Noh, and S. Cho, "Energy-efficient and low-complexity transmission control with SWIPT-NOMA for green cellular networks," *IEEE Transactions on Wireless Communications*, vol. 22, no. 12, pp. 9649–9663, Dec. 2023, doi: 10.1109/TWC.2023.3244968.

[5] R. Zhang, K. Xiong, Y. Lu, D. W. K. Ng, P. Fan, and K. B. Letaief, "SWIPT-enabled cell-free massive MIMO-NOMA networks: A machine learning-based approach," *IEEE Transactions on Wireless Communications*, vol. 23, no. 7, pp. 6701–6718, Jul. 2024, doi: 10.1109/TWC.2023.3327596.

[6] F. Zhou, Y. Wu, Y. -C. Liang, Z. Li, Y. Wang, and K. -K. Wong, "State of the Art, Taxonomy, and Open Issues on Cognitive Radio Networks with NOMA," *IEEE Wireless Communications*, vol. 25, no. 2, pp. 100-108, Apr. 2018, doi: 10.1109/MWC.2018.1700113.

[7] L. Zhang, M. Xiao, G. Wu, M. Alam, Y. -C. Liang, and S. Li, "A Survey of Advanced Techniques for Spectrum Sharing in 5G Networks," *IEEE Wireless Communications*, vol. 24, no. 5, pp. 44-51, Oct. 2017, doi: 10.1109/MWC.2017.1700069.

[8] L. Lv, J. Chen, Q. Ni, Z. Ding, and H. Jiang, "Cognitive Non-Orthogonal Multiple Access with Cooperative Relaying: A New Wireless Frontier for 5G Spectrum Sharing," *IEEE Communications Magazine*, vol. 56, no. 4, pp. 188-195, Apr. 2018, doi: 10.1109/MCOM.2018.1700687.

[9] S. Arzykulov, G. Nauryzbayev, T. A. Tsiftsis, and B. Maham, "Performance Analysis of Underlay Cognitive Radio Nonorthogonal Multiple Access Networks," *IEEE Transactions on Vehicular Technology*, vol. 68, no. 9, pp. 9318-9322, Sep. 2019, doi: 10.1109/TVT.2019.2930553.

[10] S. Arzykulov, G. Nauryzbayev, T. A. Tsiftsis, B. Maham, and M. Abdallah, "On the Outage of Underlay CR-NOMA Networks With Detect-and-Forward Relaying," *IEEE Transactions on Cognitive Communications and Networking*, vol. 5, no. 3, pp. 795-804, Sep. 2019, doi: 10.1109/TCCN.2019.2916561.
[11] Y. Liu, Z. Ding, M. Elkashlan, and J. Yuan, "Nonorthogonal Multiple Access in Large-Scale Underlay Cognitive Radio Networks," *IEEE Transactions on Vehicular Technology*, vol. 65, no. 12, pp. 10152-10157, Dec. 2016, doi: 10.1109/TVT.2016.2524694.
[12] M. Zeng, G. I. Tsiropoulos, O. A. Dobre, and M. H. Ahmed, "Power Allocation for Cognitive Radio Networks Employing Non-Orthogonal Multiple Access," in *IEEE Global Communications Conference* (GLOBECOM), Washington, DC, USA, 2016, pp. 1-5, doi: 10.1109/GLOCOM.2016.7842156.
[13] L. Lv, J. Chen, and Q. Ni, "Cooperative Non-Orthogonal Multiple Access in Cognitive Radio," *IEEE Communications Letters*, vol. 20, no. 10, pp. 2059-2062, Oct. 2016, doi: 10.1109/LCOMM.2016.2596763.
[14] M. Gupta and S. Prakriya, "Performance of CSI-Based Power Control and NOMA/OMA Switching for Uplink Underlay Networks With Imperfect SIC," *IEEE Transactions on Cognitive Communications and Networking*, vol. 8, no. 4, pp. 1753-1769, Dec. 2022, doi: 10.1109/TCCN.2022.3185076.
[15] K. K. Godugu and S. Vappangi, "Investigations on Secrecy Performance of Downlink Overlay CR-NOMA System With SIC Imperfections," *IEEE Access*, vol. 12, pp. 18051-18072, 2024, doi: 10.1109/ACCESS.2024.3361038.
[16] Y. Xiao, S. A. Tegos, P. D. Diamantoulakis, Z. Ma, and G. K. Karagiannidis, "On the Ergodic Rate of Cognitive Radio Inspired Uplink Multiple Access," *IEEE Communications Letters*, vol. 27, no. 1, pp. 95-99, Jan. 2023, doi: 10.1109/LCOMM.2022.3209930.
[17] T. Le-Thanh and K. Ho-Van, "Secured NOMA Full-Duplex Transmission With Energy Harvesting," *IEEE Access*, vol. 12, pp. 91342-91356, 2024, doi: 10.1109/ACCESS.2024.3421353.
[18] K. Agrawal, A. Jee, and S. Prakriya, "Performance of SWIPT in Cooperative Networks With Direct Link and Nonlinear Energy Harvesting at the Battery-Assisted Relay," *IEEE Transactions on Green Communications and Networking*, vol. 6, no. 2, pp. 1198-1215, Jun. 2022, doi: 10.1109/TGCN.2022.3141099.
[19] H. W. Oleiwi, N. Saeed, and H. S. Al-Raweshidy, "A Cooperative SWIPT-Hybrid-NOMA Pairing Scheme considering SIC imperfection for THz Communications," in *2022 4th Global Power, Energy and Communication Conference (GPECOM)*, Nevsehir, Turkey, 2022, pp. 638-643, doi: 10.1109/GPECOM55404.2022.9815677.
[20] Z. Na, J. Lv, M. Zhang, B. Peng, M. Xiong, and M. Guan, "GFDM Based Wireless Powered Communication for Cooperative Relay System," *IEEE Access*, vol. 7, pp. 50971-50979, 2019, doi: 10.1109/ACCESS.2019.2911176.
[21] A. Iqbal and T. -J. Lee, "Opportunistic Backscatter Communication Protocol Underlying Energy Harvesting IoT Networks," *IEEE Access*, vol. 11, pp. 89568-89580, 2023, doi: 10.1109/ACCESS.2023.3306777.
[22] K. K. Godugu, A. S. Kumar, S. Vappangi, and S. Shafi, "Energy Harvesting Enabled Overlay CR-NOMA System: Throughput and Outage Analysis," in *2024 IEEE International Conference on Electronics, Computing and Communication Technologies (CONECCT)*, Bangalore, India, 2024, pp. 1-6, doi: 10.1109/CONECCT62155.2024.10677329.
[23] F. Li, H. Jiang, R. Fan, and P. Tan, "Cognitive Non-Orthogonal Multiple Access With Energy Harvesting: An Optimal Resource Allocation Approach," in *IEEE Transactions on Vehicular Technology*, vol. 68, no. 7, pp. 7080-7095, Jul. 2019, doi: 10.1109/TVT.2019.2919261.
[24] X. Wang *et al.*, "Energy Efficiency Optimization for NOMA-Based Cognitive Radio With Energy Harvesting," *IEEE Access*, vol. 7, pp. 139172-139180, 2019, doi: 10.1109/ACCESS.2019.2940698.
[25] X. Xie *et al.*, "User selection and dynamic power allocation in the SWIPT-NOMA relay system," *EURASIP Journal on Wireless Communications and Networking*, vol. 2021, no. 1, p. 124, 2021, doi: 10.1186/s13638-021-01998-0.
[26] T.-T. Nguyen, S. Q. Nguyen, P. X. Nguyen, and Y.-H. Kim, "Evaluation of Full-Duplex SWIPT Cooperative NOMA-Based IoT Relay Networks over Nakagami-m Fading Channels," *Sensors*, vol. 22, no. 5, p. 1974, 2022, doi: 10.3390/s22051974.
[27] Z. Elsaraf, F. A. Khan, and Q. Z. Ahmed, "Deep learning based power allocation schemes in NOMA systems: A review," *arXiv preprint*, 2021, doi: 10.48550/arXiv.2108.13165.
[28] F. Jameel, W. U. Khan, Z. Chang, T. Ristaniemi, and J. Liu, "Secrecy Analysis and Learning-Based Optimization of Cooperative NOMA SWIPT Systems," in *2019 IEEE International Conference on Communications Workshops (ICC Workshops)*, Shanghai, China, 2019, pp. 1-6, doi: 10.1109/ICCW.2019.8756894.
[29] Z. Li, W. Chen, Q. Wu, K. Wang, and J. Li, "Joint Beamforming Design and Power Splitting Optimization in IRS-Assisted SWIPT NOMA Networks," *IEEE Transactions on Wireless Communications*, vol. 21, no. 3, pp. 2019-2033, Mar. 2022, doi: 10.1109/TWC.2021.3108901.
[30] Y. Xu *et al.*, "Joint Beamforming and Power-Splitting Control in Downlink Cooperative SWIPT NOMA Systems," *IEEE Transactions on Signal Processing*, vol. 65, no. 18, pp. 4874-4886, Sep. 2017, doi: 10.1109/TSP.2017.2715008.
[31] T. Manglayev, R. C. Kizilirmak, and Y. H. Kho, "AI Based Power Allocation for NOMA," *Wireless Personal Communications*, vol. 124, pp. 3253–3261, 2022, doi: 10.1007/s11277-022-09511-6.
[32] K. Kavitha and S. Vappangi, "Performance Analysis of Novel User Pairing-Based Hybrid NOMA System With Fixed/Optimal Power Allocation Strategy," *IEEE Access*, vol. 11, pp. 106037-106053, 2023, doi: 10.1109/ACCESS.2023.3319664.
[33] X. Xie, J. Liu, J. Huang, and S. Zhao, "Ergodic Capacity and Outage Performance Analysis of Uplink Full-Duplex Cooperative NOMA System," *IEEE Access*, vol. 8, pp. 164786-164794, 2020, doi: 10.1109/ACCESS.2020.3022279.
[34] Y. Zhang, Z. Yang, Y. Feng, and S. Yan, "Performance Analysis of Cooperative Relaying Systems With Power-Domain Non-Orthogonal Multiple Access," *IEEE Access*, vol. 6, pp. 39839-39848, 2018, doi: 10.1109/ACCESS.2018.2854774.
[35] I. S. Gradshteyn and I. M. Ryzhik, *Table of Integrals, Series and Products*, Elsevier, 7th edition, San Diego, Mar. 2007.
[36] H. Q. Tran, C. V. Phan, and Q. T. Vien, "Power splitting versus time switching based cooperative relaying protocols for SWIPT in NOMA systems," *Physical Communication*, vol. 41, p. 101098, 2020, doi: 10.1016/j.phycom.2020.101098.
[37] H. Q. Tran, C. V. Phan, and Q. T. Vien, "Performance analysis of power-splitting relaying protocol in SWIPT based cooperative NOMA systems," *EURASIP Journal on Wireless Communications and Networking*, vol. 1, pp. 1-26, 2021, doi: 10.1186/s13638-021-01981-9.

BIOGRAPHIES OF AUTHORS

Mr. Udari Naresh has received his B.Tech. degree in Electronics and Communication Engineering in the year 2011 from JNTU Hyderabad, India. He further pursued his academic interests by completing his Master of Technology degree in VLSI and Embedded Systems from JNTU Hyderabad in 2014. Currently, he is pursuing his Doctor of Philosophy at the School of Engineering and Technology, Bharatiya Engineering Science amd Technology Innovation University (BESTIU). Professionally, he has been serving as an Assistant Professor since 2014 at various engineering colleges in Hyderabad, India. He is currently employed at St. Mary's Engineering College in Hyderabad. His research focus areas include VLSI, performance analysis, and resource allocation in non-orthogonal multiple access (NOMA) systems, as well as cooperative NOMA, secure-NOMA, SWIPT-NOMA, and cognitive radio-based NOMA. To date, he has published five research papers in reputable journals, demonstrating his commitment to advancing knowledge in his field of expertise. He can be contacted at email: naresh.bestiu@gmail.com.

Dr. Kothapalli Sravan Abhilash has received his B.Tech. degree in Electronics and Communication Engineering from Jawaharlal Nehru Technological University Kakinada, Andhra Pradesh India in the year 2007. M.Tech. degree from Andhra University, Visakhapatnam, Andhra Pradesh, India in the year 2012. Ph.D. degree in electronic and communication engineering from Veer Bahadur Singh Purvanchal University, Uttar Pradesh, India, in the year 2021. Currently working as an Associate Professor in CMR Engineering College, Hyderabad. Research interests include wireless networks, CR, NOMA, and machine learning applications in communication. He has 3 patents, Published one book. He received 2 Awards in Teaching and Research. He has authored or coauthored more than 10 high-quality research papers in international leading journals and primer conferences. He can be contacted at email: dr.sravankothapalli@gmail.com.